The Astronomical Journal, 163:242 (11pp), 2022 May https://doi.org/10.3847/1538-3881/ac5f50

Substellar Hyades Candidates from the UKIRT Hemisphere Survey

Adam C. Schneider[1,2], Frederick J. Vrba[1], Jeffrey A. Munn[1], Scott E. Dahm[1], Justice Bruursema[1], Stephen J. Williams[1], Bryan N. Dorland[3], Jacqueline K. Faherty[4], Austin Rothermich[4], Emily Calamari[4], Michael C. Cushing[5], Dan Caselden[4], Martin Kabatnik[6], William Pendrill[6], Arttu Sainio[6], Nikolaj Stevnbak Andersen[6], and Christopher Tanner[6]

[1] United States Naval Observatory, Flagstaff Station, 10391 West Naval Observatory Road, Flagstaff, AZ 86005, USA; aschneid10@gmail.com
[2] Department of Physics and Astronomy, George Mason University, MS3F3, 4400 University Drive, Fairfax, VA 22030, USA
[3] United States Naval Observatory, 3450 Massachusetts Avenue NW, Washington, DC 20392-5420, USA
[4] Department of Astrophysics, American Museum of Natural History, Central Park West at 79th Street, New York, NY 10024, USA
[5] Ritter Astrophysical Research Center, Department of Physics and Astronomy, University of Toledo, 2801 W. Bancroft Street, Toledo, OH 43606, USA
[6] Backyard Worlds: Planet 9, USA

Received 2022 February 22; revised 2022 March 17; accepted 2022 March 18; published 2022 April 29

Abstract

We have used data from the UKIRT Hemisphere Survey to search for substellar members of the Hyades cluster. Our search recovered several known substellar Hyades members, and two known brown dwarfs that we suggest may be members based on a new kinematic analysis. We uncovered thirteen new substellar Hyades candidates, and obtained near-infrared follow-up spectroscopy of each with IRTF/SpeX. Six candidates with spectral types between M7 and L0 are ruled out as potential members based on their photometric distances ($\gtrsim$100 pc). The remaining seven candidates, with spectral types between L5 and T4, are all potential Hyades members, with five showing strong membership probabilities based on BANYAN Σ and a convergent point analysis. Distances and radial velocities are still needed to confirm Hyades membership. If confirmed, these would be some of the lowest mass free-floating members of the Hyades yet known, with masses as low as $\sim$30 M_{Jup}. An analysis of all known substellar Hyades candidates shows evidence that the full extent of the Hyades has yet to be probed for low-mass members, and more would likely be recovered with deeper photometric and astrometric investigations.

Unified Astronomy Thesaurus concepts: Low mass stars (2050); Open star clusters (1160)

Unified Astronomy Thesaurus concepts:

Brown dwarfs have central temperatures that never reach the critical threshold for stable thermonuclear H burning (Hayashi & Nakano 1963; Kumar 1963). These substellar objects thus do not form a main sequence, but instead radiatively cool over time, thereby following a mass–luminosity–age relationship. It is therefore difficult to constrain brown dwarf fundamental properties such as mass, luminosity, or age, because one of them must be known to determine the other two. Brown dwarfs with known ages, while rare, can break this degeneracy. For this reason, any brown dwarf that can be tied to a nearby young association or open cluster with a well-constrained age provides a valuable benchmark for fundamental tests of substellar theory.

The Hyades is the closest open cluster to the Sun ($\sim$47 pc; Lodieu et al. 2019). As such, it has been extensively characterized, resulting in well-determined member identification down to the substellar boundary (e.g., Röser et al. 2011; Gaia Collaboration et al. 2018; Reino et al. 2018; Lodieu et al. 2019; Smart & Sarro et al. 2021b), a well-determined age of $\sim$650 Myr (e.g., Lebreton et al. 2001; De Gennaro et al. 2009; Martín et al. 2018; Lodieu et al. 2019), and an established slightly supersolar metallicity (e.g., [Fe/H] $\sim$ 0.146 dex; Cummings et al. 2017). As the nearest open cluster, Hyades members also have significant proper motions ($\mu_{\mathrm{total}} \sim 100$ mas yr^{-1}). While some properties of the Hyades cluster, such as its distance and its relatively large proper motion, make it an ideal site for investigations of substellar populations, there are limitations to its full exploration. Being so near, Hyades members extend over a very large area of the sky, with tidal tails extending even further (Meingast & Alves 2019; Röser et al. 2019), making surveys with deep imaging of the entire cluster challenging. While large scale infrared surveys have enabled some exploration of the nearer cluster members (e.g., Pérez-Garrido et al. 2017), such surveys (e.g., 2MASS; Skrutskie et al. 2006) are not deep enough to detect substellar members with very low temperatures over the entire Hyades distance range. Despite these challenges, several L- and T-type members, as well as candidate members of the Hyades, have been identified (Bouvier et al. 2008; Hogan et al. 2008; Pérez-Garrido et al. 2017; Schneider et al. 2017; Pérez-Garrido et al. 2018; Zhang et al. 2021).

We have performed a large area search for new candidate substellar members of the Hyades using the United Kingdom Infra-Red Telescope (UKIRT) Hemisphere Survey (UHS; Dye et al. 2018), which covers the majority of the spatial extent of the Hyades. We describe our search in Section 2 and follow-up spectroscopic observations in Section 3. The analysis of our new Hyades substellar candidates is presented in Section 4, and a discussion of our results is given in Section 5.

2. Target Selection

The UHS covers approximately 12,700 deg^2 in the northern hemisphere. Combined with existing UKIDSS surveys (Lawrence et al. 2007), the UHS covers the entire northern hemisphere between 0° and 60°. The *J*-band portion of the survey has been publicly released (Dye et al. 2018), and the *K*-band survey has an anticipated public release some time in 2023.

We constructed a proper motion catalog based on UHS data by cross-matching each *K*-band UHS detection with the UHS

Table 1
Recovered Substellar Hyades Members

CWISE Name	Disc. References	μ_α (mas yr^{-1})	μ_δ (mas yr^{-1})	$J_{\rm UHS}$[a] (mag)	$K_{\rm UHS}$[a] (mag)	SpT	SpT References
J035304.34+041820.0[b]	1	171.2 ± 3.1	35.8 ± 2.9	16.312 ± 0.013	14.509 ± 0.010	L6pec (red)	1
J041232.79+104408.0[c]	2	129.5 ± 3.8	−5.5 ± 3.5	17.471 ± 0.041	15.263 ± 0.019	L5: (red)	2
J041733.97+143015.2	3	123.6 ± 2.7	−17.8 ± 2.3	16.468 ± 0.015	14.625 ± 0.011	L2[d]	4
J041835.00+213126.6	5	142.0 ± 4.3	−51.8 ± 4.0	17.203 ± 0.027	15.195 ± 0.015	L5	5
J042418.72+063745.5	6	138.8 ± 2.8	7.5 ± 2.9	17.222 ± 0.022	15.434 ± 0.019	L4	6
J043038.87+130956.7	7	141.6 ± 3.5	−21.5 ± 3.6	16.869 ± 0.017	16.199 ± 0.037	T2.5	8
J043543.04+132344.8	3	95.7 ± 3.9	−17.7 ± 3.4	16.714 ± 0.016	14.892 ± 0.012	L6 (red)[e]	9
J043642.79+190134.6	2	113.5 ± 2.0	−42.1 ± 2.0	16.766 ± 0.017	14.849 ± 0.013	L6	2
J043803.58+070055.2	6	88.7 ± 3.1	3.1 ± 3.1	16.778 ± 0.018	14.993 ± 0.014	L1	6
J043855.29+042300.6	10	118.7 ± 3.5	11.7 ± 3.4	16.381 ± 0.012	15.108 ± 0.016	T2	10
J044105.60+213001.3	2	98.7 ± 4.6	−48.5 ± 4.4	17.441 ± 0.032	15.352 ± 0.021	L5 (red)	2
J044635.44+145125.7	3	79.1 ± 2.6	−22.4 ± 2.5	16.378 ± 0.015	14.594 ± 0.009	L3.5	11

Notes.
[a] Based on the UKIRT photometric system (Hodgkin et al. 2009).
[b] CWISE J035304.34+041820.0 has not been suggested as a potential Hyades member before this work.
[c] CWISE J041232.79+104408.0 was suggested to be an unlikely Hyades member in Schneider et al. (2017), though we find it to be high-probability member using more precise astrometry.
[d] Lodieu et al. (2014) report an optical spectral type of L1 for this object, while Martín et al. (2018) found an optical spectral type of L3.5. Lodieu et al. (2019) gives a spectral type of L2, and we adopt that type here.
[e] Lodieu et al. (2014) found an optical spectral type of L3.5 for this object.
References. (1) Kellogg et al. (2017); (2) Schneider et al. (2017); (3) Hogan et al. (2008); (4) Lodieu et al. (2019); (5) Pérez-Garrido et al. (2017); (6) Pérez-Garrido et al. (2018); (7) Bouvier et al. (2008); (8) Liu et al. (2016); (9) Best et al. (2015); (10) Best et al. (2020); (11) Martín et al. (2018).

J-band catalog, after first removing those sources from each UHS catalog with matches in Gaia EDR3 (Gaia Collaboration et al. 2021a). The *J*-/*K*-band matching was done with incrementally increasing matching radii. For each match, a preliminary proper motion was calculated by differencing the *J*- and *K*-band positions. Matches were kept only if the *K*-band detection had a corresponding entry in CatWISE 2020 (Marocco et al. 2021), after propagating the *K*-band position to the CatWISE 2020 epoch using the preliminary proper motion. Final proper motions were calculated based on the *J*- and *K*-band positions, as well as the Pan-STARRS (PS1) DR2 (Chambers et al. 2016; Magnier et al. 2020) position for those objects with a match in the Pan-STARRS catalog.

Recent studies using Gaia data have led to the discovery of Hyades tidal tails (Meingast & Alves 2019; Röser et al. 2019). The identification of members of the Hyades tidal tails necessitated a spatial density filter, which requires accurate distances. Since we expect any new candidates found through our search to be beyond Gaia magnitude limits, we focus our search for substellar Hyades candidates around the cluster center and omit the recently discovered Hyades tidal tails. To select candidates from our UHS proper motion catalog, we limit our search to objects within 18 pc of the cluster center, which should include all bound and halo cluster members (Lodieu et al. 2019). To do this, we imposed R.A. and decl. constraints based on the extremes of known halo Hyades members from the Gaia Catalogue of Nearby Stars (GCNS; Smart & Sarro et al. 2021b). Note that the Smart & Sarro et al. (2021b) census includes 560 of the 568 Hyades members within 18 pc of the cluster center found in Lodieu et al. (2019). Specifically, we required $46 \leqslant$ R.A. (deg) $\leqslant 85$ and $-4.5 \leqslant$ decl. (deg) $\leqslant 38.5$. We also ensured each candidate had proper motion components consistent with known Hyades members from Lodieu et al. (2019) by imposing proper motion constraints based on these same members: $42 \leqslant \mu_\alpha$ (mas yr^{-1}) $\leqslant 197$ and $-92 \leqslant \mu_\delta$ (mas yr^{-1}) $\leqslant 43$. To identify substellar candidates, we select only sources with *J*-W2 colors >1.5 mag, which is inclusive of the vast majority of L- and T-type brown dwarfs (see e.g., Figure 7 of Kirkpatrick et al. 2016). We also chose a *J*-band magnitude limit of 17.5 mag, which corresponds to the approximate limit of what is observable with the SpeX spectrograph (Rayner et al. 2003) in prism mode at NASA's Infrared Telescope Facility (see Section 3). Over 450 candidates were selected via these criteria.

We verified each source was a kinematic match to the Hyades using the BANYAN Σ classifier (Gagné et al. 2018), keeping those with a nonzero probability of membership in the Hyades. BANYAN Σ uses sky positions, proper motions, and, when available, radial velocities and distances to determine the probability that a given object is a member of any nearby young association or cluster using Bayesian statistics. There were 105 objects that returned a nonzero BANYAN Σ probability of belonging to Hyades. A visual inspection of each object further reduced the number of candidates to 25, where candidates removed via visual inspection were typically blended or extended objects.

2.1. Recovered Substellar Hyades Candidates

Of the remaining 25 candidates, 11 were previously suggested substellar Hyades members from Bouvier et al. (2008), Hogan et al. (2008), Pérez-Garrido et al. (2017), Schneider et al. (2017), Pérez-Garrido et al. (2018), and Zhang et al. (2021). Details of these recovered members are listed in Table 1.

One object recovered by our search was CWISE J041232.79+104408.0 (WISEA J041232.77+104408.3; Schneider et al. 2017). CWISE J041232.79+104408.0 was discovered in Schneider et al. (2017) with a spectral type of L5: (red), and was considered an unlikely Hyades member based on a crude proper motion and a comparison with known Hyades members at that time. Our measured proper motion components for this source have smaller uncertainties than the Schneider et al. (2017) values by a factor of ∼10 (see Table 1). We therefore reevaluate this object's potential membership based on these updated values and BANYAN Σ and find a 96.2% probability of Hyades membership.

We further test the potential Hyades membership of CWISE J041232.79+104408.0 by evaluating whether or not its proper motion is consistent with the Hyades convergent point, defined in Madsen et al. (2002). Following Hogan et al. (2008), we compare the proper motion angle (θ_{μ}) and the angle measured between a line pointing north and a line from CWISE J041232.79+104408.0 to the convergent point (θ_{cp}), which should be similar for Hyades members. We find $\theta_{\mu} = 92^{\circ}.4$ and $\theta_{cp} = 93^{\circ}.6$. Considering our proper motion precisions, these angles are discrepant by $<1\sigma$. We can also use the measured proper motion of CWISE J041232.79+104408.0 and the moving cluster method to estimate a distance to this object if it were a Hyades member. Using the cluster velocity of 46.38 km s^{-1} from Lodieu et al. (2019), we find a distance of 42.2 pc, which agrees well with this object's photometric distance estimate of 46 ± 6 pc from Schneider et al. (2017). We thus reclassify CWISE J041232.79+104408.0 as a likely Hyades member.

Another object recovered by our search was CWISE J043803.58+070055.2 (2M0438+0700), which was suggested as a Hyades candidate in Pérez-Garrido et al. (2018), with a spectral type of L1. Using their spectral type and our *K*-band magnitude for this source, we find a photometric distance of ∼77 pc, which is much larger than the ∼44 pc distance estimate from Pérez-Garrido et al. (2018). If CWISE J043803.58+070055.2 is ∼77 pc distant, it is >30 pc from the Hyades cluster center. One possible explanation that would bring CWISE J043803.58+070055.2 closer to the cluster center is a later spectral type, as the spectrum used to type this object in Pérez-Garrido et al. (2018) covers a limited wavelength range and has a low signal-to-noise ratio (S/N). A high S/N spectrum of this source may be warranted. We include it in Table 1 as a possible Hyades member for completeness.

2.2. Other Recovered Brown Dwarfs

We also recovered the known brown dwarf CWISE J035304.34+041820.0 (2MASS J03530419+0418193; Kellogg et al. 2017). CWISE J035304.34+041820.0 is an extremely red L dwarf discovered in Kellogg et al. (2017), which has not been linked to the Hyades previously. Many known, young brown dwarfs appear redder than field-age counterparts with similar spectral types (e.g., Faherty et al. 2016). And while CWISE J035304.34+041820.0 is extremely red compared to other objects with an L6 spectral type, Kellogg et al. (2017) noted that this source did not display any spectroscopic signatures of youth. The low-gravity features used to diagnose young ages for brown dwarfs are calibrated for ages $\lesssim$200 Myr (e.g., Allers & Liu 2013), and therefore the lack of youthful features in the spectrum of CWISE J035304.34+041820.0 does not rule out Hyades membership.

Using our measured proper motion for this source from Table 1, we find a 14.7% chance of belonging to the Hyades cluster from BANYAN Σ and a kinematic distance assuming Hyades membership of ∼34 pc. Schneider et al. (2016) found that *K*-band photometric distances show good agreement with measured parallaxes for exceptionally red objects, especially compared to other photometric bands. Using the absolute *K*-band magnitude versus spectral type relation from Dupuy & Liu (2012) and the UHS *K*-band magnitude for this source, we find a photometric distance of ∼31 pc, in good agreement with the kinematic distance estimate. At a distance of ∼31 pc, CWISE J035304.34+041820.0 would be ∼19 pc from the Hyades cluster center given in (Lodieu et al. 2019), just beyond the halo region defined in that work (18 pc).

As with CWISE J041232.79+104408.0, we compared the proper motion angle of CWISE J035304.34+041820.0 to the convergent point angle and found $\theta_{\mu} = 78^{\circ}.2$ and $\theta_{cp} = 84^{\circ}.4$. Considering our proper motion precisions, these angles are discrepant by $\sim 3\sigma$. Using the moving cluster method, we find a kinematic distance of 35.2 pc. This distance matches reasonably well with our photometric distance estimate of 31 pc. We therefore consider 2MASS J03530419+0418193 a potential Hyades member. A parallax and radial velocity for this source would help to firmly establish Hyades membership.

2.3. New Substellar Hyades Candidates

The remaining 13 candidates are listed in Table 2, which includes photometry from UHS (Dye et al. 2018), CatWISE 2020 (Marocco et al. 2021), and PS1 DR2 (Chambers et al. 2016; Magnier et al. 2020). We show the positions of these 13 candidates compared to known cluster and halo Hyades members from Smart & Sarro et al. (2021b) and our recovered substellar members from Table 1 in Figure 1. We note here that five of these thirteen candidates were independently discovered by citizen scientists working with the Backyard Worlds: Planet 9 project (Kuchner et al. 2017). These citizen scientists are recognized in the table notes of Table 2.

3. Observations

3.1. IRTF/SpeX

We obtained near-infrared spectra of our 13 substellar Hyades candidates with the SpeX spectrograph (Rayner et al. 2003) at NASA's 3 m Infrared Telescope Facility (IRTF) on UT 2021 Nov 11 and 12. The observations were taken in prism mode with the $0''.8$ slit, which gives a spectral resolution of $\lambda/\Delta\lambda \approx 150$ across the 0.8–2.4 μm wavelength range. A0 stars were observed immediately after each target for telluric correction purposes. Because these observations were concentrated on the Hyades, some A0 star observations were suitable for multiple targets. Depending on the brightness of the target, we took between two and sixteen images of 180 s each in an ABBA pattern with the slit aligned to the parallactic angle. Calibration files were taken between the target and the telluric observations, and the spectral extraction, wavelength calibration, and telluric correction were performed with the SpeXTool package (Vacca et al. 2003; Cushing et al. 2004). Details of the observations can be found in Table 3, and the final, reduced spectra are shown in Figure 2. We also give the S/N at the *J*-band peak for our reduced spectra in Table 3.

4. Analysis

4.1. Spectral Types

Spectral types for each candidate were determined by comparing *J*-band morphologies to near-infrared spectral

Table 2
New Substellar Hyades Candidates

CWISE Name	μ_α (mas yr^{-1})	μ_δ (mas yr^{-1})	$i_{\rm PS1}$ (mag)	$z_{\rm PS1}$ (mag)	$y_{\rm PS1}$ (mag)	$J_{\rm UHS}$[a] (mag)	$K_{\rm UHS}$[a] (mag)	W1 (mag)	W2 (mag)
J031042.59+204629.3[b]	164.7 ± 2.2	−27.7 ± 2.2	20.702 ± 0.031	19.240 ± 0.013	18.228 ± 0.013	15.956 ± 0.011	14.267 ± 0.009	13.723 ± 0.014	13.435 ± 0.013
J033817.87+171744.1[c]	152.0 ± 3.5	−25.3 ± 3.3	...	20.789 ± 0.075	19.707 ± 0.034	17.311 ± 0.026	15.185 ± 0.015	14.315 ± 0.016	13.910 ± 0.015
J040136.03+144454.6	99.3 ± 3.3	−18.2 ± 2.6	20.860 ± 0.048	19.512 ± 0.027	18.604 ± 0.022	16.840 ± 0.025	15.706 ± 0.028	15.512 ± 0.023	15.314 ± 0.041
J041424.22+093223.5	114.5 ± 3.6	−9.8 ± 3.5	21.052 ± 0.067	19.814 ± 0.029	18.948 ± 0.038	17.274 ± 0.035	16.278 ± 0.045	15.945 ± 0.028	15.654 ± 0.053
J041953.55+203628.0[d]	109.4 ± 9.0	−35.8 ± 8.9	...	...	19.827 ± 0.081	17.290 ± 0.029	16.990 ± 0.078	16.243 ± 0.032	15.390 ± 0.040
J042731.38+074344.9[e]	114.3 ± 3.5	5.5 ± 3.1	...	20.555 ± 0.031	19.496 ± 0.066	17.188 ± 0.025	15.302 ± 0.019	14.242 ± 0.016	13.875 ± 0.015
J043018.70+105857.1	106.3 ± 6.9	−10.7 ± 6.9	...	21.034 ± 0.182	19.903 ± 0.143	17.451 ± 0.027	17.313 ± 0.115	16.855 ± 0.050	15.828 ± 0.062
J043941.41+202514.8	80.8 ± 8.0	−30.3 ± 7.9	...	21.594 ± 0.185	19.844 ± 0.123	17.453 ± 0.027	17.196 ± 0.101	16.451 ± 0.038	15.464 ± 0.043
J044603.23+175930.8	77.3 ± 5.1	−28.8 ± 4.7	21.440 ± 0.050	19.993 ± 0.042	19.205 ± 0.033	17.453 ± 0.024	16.418 ± 0.049	15.897 ± 0.027	15.571 ± 0.050
J044747.32+082552.0	66.2 ± 3.5	−5.3 ± 3.6	21.090 ± 0.058	19.772 ± 0.024	18.854 ± 0.023	16.956 ± 0.024	15.782 ± 0.030	15.433 ± 0.022	15.144 ± 0.033
J045712.03+183344.1	61.0 ± 2.5	−28.0 ± 2.6	21.256 ± 0.040	19.847 ± 0.046	19.002 ± 0.028	17.254 ± 0.025	16.132 ± 0.037	15.910 ± 0.029	15.751 ± 0.054
J045821.05+053244.5	72.1 ± 2.8	9.4 ± 2.7	20.831 ± 0.027	19.476 ± 0.024	18.457 ± 0.019	16.600 ± 0.016	15.440 ± 0.022	15.125 ± 0.020	14.929 ± 0.027
J053204.60+111955.1[f]	72.4 ± 1.9	−30.2 ± 1.9	21.257 ± 0.053	19.420 ± 0.033	18.366 ± 0.032	15.944 ± 0.009	13.932 ± 0.006	13.193 ± 0.015	12.764 ± 0.011

Notes.
[a] Based on the UKIRT photometric system (Hodgkin et al. 2009).
[b] CWISE J031042.59+204629.3 was independently discovered by citizen scientist Nikolaj Stevnbak.
[c] CWISE J033817.87+171744.1 was independently discovered by citizen scientists Christopher Tanner, Sam Goodman, and Martin Kabatnik.
[d] CWISE J041953.55+203628.0 was independently discovered by citizen scientist Martin Kabatnik.
[e] CWISE J042731.38+074344.9 was independently discovered by citizen scientists Dan Caselden and Billy Pendrill.
[f] CWISE J053204.60+111955.1 was independently discovered by citizen scientists Arttu Sainio and Sam Goodman.

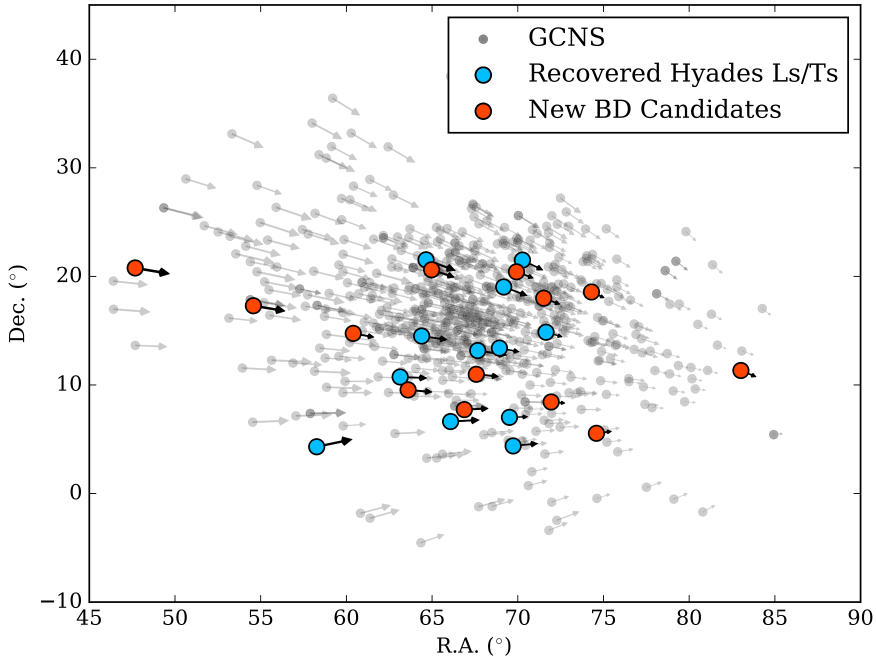

Figure 1. The J2000 positions and proper motion vectors of our substellar Hyades candidates (red) and known, recovered L- and T-type members of the Hyades (blue) compared to all known Hyades members within the halo radius (18 pc) from the GCNS (Smart & Sarro et al. 2021b).

Table 3
IRTF Observations

CWISE Name	Obs. Date (UT)	Total Exp. Time (s)	A0 Star	Spec. Type	$(S/N)_J$
J031042.59+204629.3	2021 Nov 11	1440	HD19600	L5	81
J033817.87+171744.1	2021 Nov 11	2160	HD 35036	L7	45
J040136.03+144454.6	2021 Nov 11	2160	HD 35036	M8	62
J041424.22+093223.5	2021 Nov 11	2880	HD 35036	M7	39
J041953.55+203628.0	2021 Nov 11	2880	HD 35036	T4	29
J042731.38+074344.9	2021 Nov 12	900	HD 31411	L7	33
J043018.70+105857.1	2021 Nov 12	1260	HD 35036	T3	34
J043941.41+202514.8	2021 Nov 12	1080	HD 35036	T3	31
J044603.23+175930.8	2021 Nov 12	1080	HD 35036	M7	19
J044747.32+082552.0	2021 Nov 12	1080	HD 35036	M9	38
J045712.03+183344.1	2021 Nov 12	1080	HD 35036	M8	26
J045821.05+053244.5	2021 Nov 11	1800	HD 31411	L0	27
J053204.60+111955.1	2021 Nov 11	360	HD 31411	L7	27

standards from Burgasser et al. (2006) and Kirkpatrick et al. (2010). We use standard χ^2 fitting to determine the best fitting standards, and confirm each by eye. The best fitting spectral types are given in Table 3 and the best matching near-infrared spectral standards are shown in Figure 2. As seen in the table, all candidates have spectral types of M7 or later, with the latest spectral types being T3 and T4.

4.2. Distances

None of our Hyades candidates have detections or distance measurements from Gaia (Gaia Collaboration et al. 2021a) or any other astrometric study. We use the absolute magnitude versus spectral-type relations from Dupuy & Liu (2012) and our UHS *J*- and *K*-band photometry to find distance ranges for each of our Hyades candidates, including a spectral type subclass uncertainty of ± 0.5. Distance ranges for each candidate are given in Table 4.

4.3. Hyades Membership

We evaluate our sample for Hyades membership using several methods. We first use the BANYAN Σ software (Gagné et al. 2018) using only our measured proper motions from Table 2 and the positions of each object. We then use the BANYAN Σ classifier with our photometric distance ranges as an input parameter. BANYAN Σ probabilities are given in Table 4. For the six objects that have spectral types earlier than L0 (CWISE J040136.03+144454.6, CWISE J041424.22+093223.5, CWISE J044603.23+175930.8, CWISE J044747.32+082552.0, CWISE J045712.03+183344.1, and CWISE J053204.60+111955.1), their BANYAN Σ Hyades membership probabilities drop to 0% when their photometric distances are included. This is not surprising given that their photometric distance estimates are all $\gtrsim$100 pc, well beyond the furthest known Hyades cluster members. We consider all of these objects nonmembers, and discuss them further in Section 5.1.

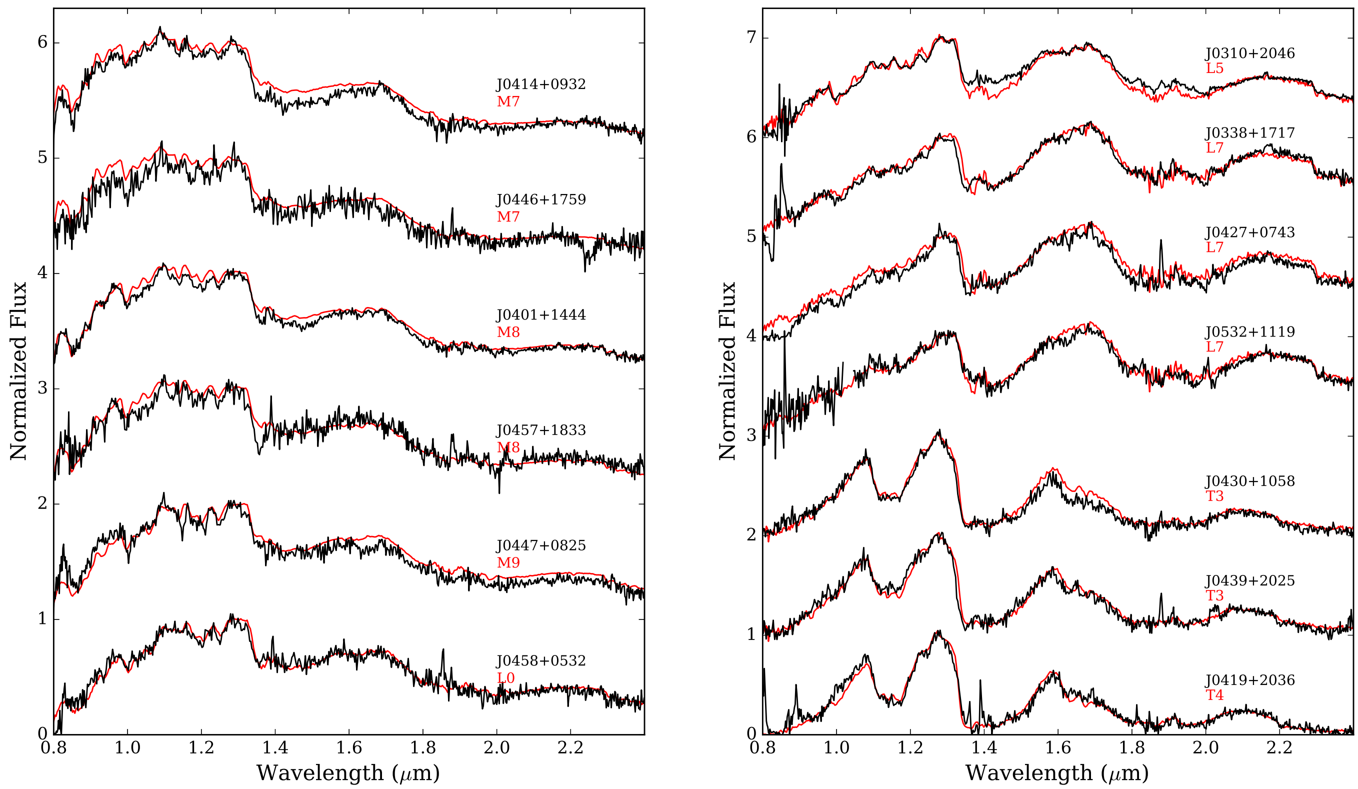

Figure 2. IRTF/SpeX spectra (black) compared to spectral standards (red). The spectra are normalized between 1.27 and 1.29 μm and offset by integer values for clarity. The spectral standards are: VB 8 (M7; Burgasser et al. 2008); VB 10 (M8; Burgasser et al. 2004); LHS 2924 (M9; Burgasser & McElwain 2006); 2MASP J0345432+254023 (L0; Burgasser & McElwain 2006); SDSS J083506.16+195304.4 (L5; Chiu et al. 2006); 2MASSI J0103320+193536 (L7; Cruz et al. 2004); 2MASS J12095613−1004008 (T3; Burgasser et al. 2004); and 2MASSI J2254188+312349 (T4; Burgasser et al. 2004).

Table 4
Hyades Membership Summary

CWISE Name	Spec. Type	$\mathrm{dist_{phot}}$ (pc)	$\mathrm{dist_{cp}}$ (pc)	$\mathrm{dist_{BANYAN}}$ (pc)	θ_{μ} (°)	θ_{cp} (°)	BANYAN[a] (%)	BANYAN[a] (%)	Member?
J031042.59+204629.3	L5	29–36	45.2	45.2	99.6	98.7	47.7	29.6	Y?
J033817.87+171744.1	L7	33–46	43.6	43.1	99.5	98.6	83.6	89.3	Y
J040136.03+144454.6	M8	134–157	58.9	56.4	100.4	98.2	28.1	0.0	N
J041424.22+093223.5	M7	185–253	47.4	47.1	94.9	91.9	64.2	0.0	N
J041953.55+203628.0	T4	34–41	48.2	46.9	108.1	109.0	93.3	96.7	Y
J042731.38+074344.9	L7	35–43	43.4	42.3	87.3	89.6	90.0	97.7	Y
J043018.70+105857.1	T3	41–53	45.7	45.3	95.8	95.4	94.4	98.2	Y
J043941.41+202514.8	T3	41–51	56.8	51.8	110.6	113.1	62.0	91.9	Y
J044603.23+175930.8	M7	201–274	55.2	53.2	110.4	110.5	81.9	0.0	N
J044747.32+082552.0	M9	125–143	63.3	57.2	94.6	91.7	23.9	0.0	N
J045712.03+183344.1	M8	160–190	62.8	59.4	114.7	114.5	27.6	0.0	N
J045821.05+053244.5	L0	98–109	52.3	49.1	82.6	85.4	31.5	0.0	N
J053204.60+111955.1	L7	19–24	32.2	31.2	112.6	106.2	7.1	34.2	Y?

Note.
[a] The first BANYAN Hyades membership probability listed does not include a distance estimate as a constraint, while the second uses the photometric distance to calculate the probability of Hyades membership.

Both CWISE J031042.59+204629.3 and CWISE J053204.60+111955.1 have relatively small Hyades membership probabilities from BANYAN Σ (<50%), with or without the inclusion of their photometric distance estimates. We consider both objects possible Hyades members based on their BANYAN Σ probabilities.

For the remaining five objects, their already high (>60%) Hyades membership probabilities from BANYAN Σ increased when their photometric distance estimates were included in their evaluation. We consider all of these objects strong Hyades candidate members based on their BANYAN Σ analysis.

We also evaluate each candidate's potential Hyades membership using their measured astrometry compared to the Hyades convergent point. As with CWISE J035304.34+041820.0 and CWISE J041232.79+104408.0 in Section 2.2, we calculate each candidate's proper motion angle (θ_{μ}) and convergent point angle (θ_{cp}). These are provided in Table 4. All angles are consistent to within $\pm 3°$ for each object, the one exception being CWISE J053204.60+111955.1, which has a proper motion angle of $112\overset{\circ}{.}6$ and a convergent point angle of $106\overset{\circ}{.}2$. Our typical proper motion uncertainty is ± 4 mas yr^{-1}, which corresponds to a

Table 5
Physical Properties on New Hyades Candidates

CWISE Name	Spec. Type	$T_{\rm eff}$ (K)	Mass[a] ($M_{\rm Jup}$)	Mass[b] ($M_{\rm Jup}$)
J031042.59+204629.3	L5	1610 ± 140	55^{+6}_{-8}	49 ± 6
J033817.87+171744.1	L7	1420 ± 140	46^{+7}_{-12}	41^{+6}_{-5}
J041953.55+203628.0	T4	1180 ± 80	28^{+4}_{-2}	32 ± 3
J042731.38+074344.9	L7	1420 ± 140	46^{+7}_{-12}	41^{+6}_{-5}
J043018.70+105857.1	T3	1200 ± 80	30^{+5}_{-3}	33 ± 3
J043941.41+202514.8	T3	1200 ± 80	30^{+5}_{-3}	33 ± 3
J053204.60+111955.1	L7	1420 ± 140	46^{+7}_{-12}	41^{+6}_{-5}

Notes.
[a] Masses determined using the hybrid models of Saumon & Marley (2008).
[b] Masses determined using the models of Phillips et al. (2020).

proper motion angle uncertainty of $\pm 2\overset{\circ}{.}3$, making a range of $\pm 7°$ equivalent to $\pm 3\sigma$. The angle difference for CWISE J053204.60+111955.1 is just within this range, and it is thus not ruled out as a candidate.

We also include the convergent point distance, and BANYAN Σ predicted distances in Table 4. For the seven objects with BANYAN Σ probabilities greater than 0% when photometric distances are included, the photometric distances, convergent point distances, and BANYAN Σ predicted distances are reasonably consistent. For CWISE J053204.60+111955.1, if it is a Hyades member, it is well outside the halo radius of the cluster. Using a photometric distance estimate of ∼20 pc, CWISE J053204.60+111955.1 is ∼28 pc from the *xyz* position of the cluster center given in Lodieu et al. (2019). Lodieu et al. (2019) and Smart & Sarro et al. (2021b) identified over 100 Hyades cluster members between 18 and 30 pc from the cluster center, so Hyades membership for CWISE J053204.60+111955.1 cannot be ruled out. Regardless, CWISE J053204.60+111955.1 has a photometric distance estimate suggesting that it may be part of the 20 pc sample of nearby stars and brown dwarfs.

4.4. Physical Properties

Previous studies have shown that field-age and young brown dwarfs with similar spectral types have significantly different effective temperatures (e.g., Filippazzo et al. 2015). However, these investigations have generally compared field-age brown dwarfs to brown dwarfs with ages ≲200 Myr. Liu et al. (2016) showed that the T2.5 Hyades member CFHT-Hy-20 (CWISE J043038.87+130956.7) had infrared photometry consistent with the field population. Thus when estimating effective temperatures for our sample, we use the relation from Kirkpatrick et al. (2021) for field-age brown dwarfs. We include a ±0.5 subtype uncertainty for spectral type.

To estimate masses, we use two sets of models; the hybrid models from Saumon & Marley (2008) and those from Phillips et al. (2020). Uncertainties are found in a Monte Carlo fashion, where we assume a normal age distribution around 650 ± 50 Myr for each object. Masses and effective temperatures for each potential Hyades member are given in Table 5. The model-estimated masses for each of our seven possible Hyades members are all below 50 $M_{\rm Jup}$, firmly in the substellar regime. Our new T-type candidate members all have masses ∼30 $M_{\rm Jup}$, which puts them among the lowest masses of candidate Hyades members.

Previously suggested T-type Hyades members include CFHT-Hy-20 and CFHT-Hy-21 (Bouvier et al. 2008), with spectral types of T2.5 and T1, respectively (Bouvier et al. 2008; Liu et al. 2016); and PSO J049.1159+26.8409, PSO J052.2746+13.3754, and PSO J069.7303+04.3834 (Zhang et al. 2021), with spectral types of T2.5, T3.5, and T2, respectively (Best et al. 2015, 2020). Zhang et al. (2021) also suggested the known T6.5 brown dwarf WISEPA J030724.57+290447.6 (Kirkpatrick et al. 2011) as a potential Hyades member, but we rule out Hyades membership for this object in Section 5.2. Because spectral type scales with mass for substellar objects with the same age, and CWISE J041953.55+203628.0 has the latest spectral type of candidate Hyades members (T4), it is likely the lowest mass free-floating Hyades member yet known.

5. Discussion

5.1. What about Those Distant Late-Ms/Early-Ls with Hyades Proper Motions?

Our search returned six late-M- or early-L- type objects with Hyades-like proper motions that have photometric distance measurements well beyond the nominal cluster radius. While it is intriguing to consider these objects as part of a potential extended Hyades stream, their significant proper motions at their estimated distances suggest very different space velocities than known Hyades members. Using their photometric distances and proper motions, we find tangential velocity ($V_{\rm tan}$) values ranging from 36 km s^{-1} for CWISE J045821.05+053244.5 to 120 km s^{-1} for CWISE J041424.22+093223.5, many of which are consistent with the thick disk or halo population of the Milky Way (e.g., Bensby et al. 2003). For Hyades members within the halo radius of 18 pc from Smart & Sarro et al. (2021b), we find an average $V_{\rm tan}$ of 24 ± 4 km s^{-1}. We conclude that all of these objects are likely unrelated to the Hyades and are therefore background interlopers.

5.2. The Current Census of Substellar Hyades Members

There have been several relatively recent attempts to identify substellar Hyades members (e.g., Pérez-Garrido et al. 2018; Zhang et al. 2021). We took this opportunity to combine the results of these efforts with our search to examine the completeness of these combined investigations. One might expect a different distance distribution for substellar Hyades members than stellar members, as efforts to identify substellar members are typically magnitude limited in some way. This is either because of the specific data set being used to identify candidates, or other considerations, such as the $J < 17.5$ mag criterion we imposed in our search to facilitate follow-up observations. To investigate this, we sought to compare the distance distribution of known Hyades members from Smart & Sarro et al. (2021b) with known and suspected substellar Hyades members. For the known Hyades members, we use the list of 713 suggested members from Smart & Sarro et al. (2021b) within 30 pc of the Hyades cluster center. We do not limit to the 18 pc halo radius as we did with our specific UHS brown dwarf search because previous surveys for substellar members have various selection criteria. Therefore, the full 713 member sample will return a more consistent comparison.

For the substellar Hyades sample, we include all suspected Hyades members with spectral types of L0 or later, which corresponds to a mass of 72 $M_{\rm Jup}$ at the age of the Hyades using the evolutionary models of Phillips et al. (2020). We use 11

Table 6
Substellar Hyades Members and Candidate Members

CWISE Name	Other Name	Disc. References	SpT	SpT References	μ_α (mas yr^{-1})	μ_δ (mas yr^{-1})	μ References	Dist.[a] (pc)	Dist. References	Mass ($M_{\rm Jup}$)	BANYAN (%)
J031042.59+204629.3	...	1	L5	1	164.7 ± 2.2	-27.7 ± 2.2	1	[32]	1	49 ± 6	47.7
J031627.87+265027.2	PSO J049.1159+26.8409	2	T2.5	2	201.1 ± 2.4	-52.8 ± 1.9	3	29.9 ± 2.8	3	33 ± 3	85.6
J032905.95+132231.5	PSO J052.2746+13.3754	3	T3.5	3	273.2 ± 2.0	-20.7 ± 2.0	3	22.6 ± 1.5	3	33 ± 3	92.5
J033817.87+171744.1	...	1	L7	1	152.0 ± 3.5	-25.3 ± 3.3	1	[35]	1	41^{+6}_{-5}	83.6
J035246.42+211232.7	Hya02	4	L1.5	5	116.4 ± 2.0	-26.9 ± 1.5	6	56.5 ± 6.4	6	65 ± 6	24.4
J035304.34+041820.0	2MASS J03530419+0418193	7	L6pec (red)	7	171.2 ± 3.1	35.8 ± 2.9	1	[31]	1	45 ± 6	14.7
J035542.11+225700.9	Hya11	4	L3	8	164.4 ± 3.0	-41.1 ± 2.3	9	25.6 ± 10.7	6	58 ± 6	82.0
J041024.02+145910.1	Hya03	4	L0.5	5	110.2 ± 1.4	-13.1 ± 1.3	10	55.9 ± 3.7	10	70 ± 6	72.6
J041232.79+104408.0	WISEA J041232.77+104408.3	11	L5: (red)	11	129.5 ± 3.8	-5.5 ± 3.5	1	[46]	11	49 ± 6	96.2
J041733.97+143015.2	Hya10	4	L2[b]	6	123.6 ± 2.7	-17.8 ± 2.3	1	35.1 ± 4.8	6	62 ± 6	99.2
J041835.00+213126.6	2MASS J04183483+2131275	12	L5	12	141.5 ± 2.7	-45.7 ± 2.3	6	38.8 ± 4.4	6	49 ± 6	98.3
J041953.55+203628.0	...	1	T4	1	109.4 ± 9.0	-35.8 ± 8.9	1	[37]	1	32 ± 3	93.3
J042418.72+063745.5	2M0424+0637	13	L4	13	138.8 ± 2.8	7.5 ± 2.9	1	[64]	1	53 ± 6	93.4
J042731.38+074344.9	...	1	L7	1	114.3 ± 3.5	5.5 ± 3.1	1	[37]	1	41^{+6}_{-5}	90.0
J042922.88+153529.4	CFHT-Hy-21	14	T1	14	82.1 ± 9.8	-15.5 ± 8.6	6	29.9 ± 11.3	6	34 ± 3	74.7
J043018.70+105857.1	...	1	T3	1	106.3 ± 6.9	-10.7 ± 6.9	1	[49]	1	33 ± 3	94.4
J043038.87+130956.7	CFHT-Hy-20	14	T2.5	15	142.6 ± 1.6	-16.5 ± 1.7	15	32.5 ± 1.6	15	33 ± 3	98.7
J043543.04+132344.8	Hya12	4	L6 (red)[c]	2	100.2 ± 1.9	-15.1 ± 2.0	6	41.5 ± 3.6	6	45 ± 6	99.5
J043642.79+190134.6	WISEA J043642.75+190134.8	11	L6	11	113.5 ± 2.0	-42.1 ± 2.0	1	[35]	11	45 ± 6	96.2
J043855.29+042300.6	PSO J069.7303+04.3834	3	T2	3	118.7 ± 3.5	11.7 ± 3.4	1	27.3 ± 4.3	3	34 ± 3	86.0
J043941.41+202514.8	...	1	T3	1	80.8 ± 8.0	-30.3 ± 7.9	1	[47]	1	33 ± 3	62.0
J044105.60+213001.3	WISEA J044105.56+213001.5	11	L5 (red)	11	98.7 ± 4.6	-48.5 ± 4.4	1	[45]	11	49 ± 6	90.5
J044635.44+145125.7	Hya19	4	L3.5	5	79.1 ± 2.6	-22.4 ± 2.5	1	48.5 ± 5.9	6	55 ± 6	98.5
J045845.76+121234.1	Hya08	4	L0.5	5	88.6 ± 1.1	-17.5 ± 0.8	10	44.0 ± 1.7	10	70 ± 6	99.0
J053204.60+111955.1	...	1	L7	1	72.4 ± 1.9	-30.2 ± 1.9	1	[20]	1	41^{+6}_{-5}	7.1

Notes.
[a] Distances in square brackets are photometric distances. All other distances come from measured parallaxes.
[b] Lodieu et al. (2014) report an optical spectral type of L1 for this object, while Martín et al. (2018) found an optical spectral type of L3.5. Lodieu et al. 2019 gives a spectral type of L2, and we adopt that type here.
[c] Lodieu et al. (2014) found an optical spectral type of L3.5 for this object.

References (1) This work; (2) Best et al. (2015); (3) Best et al. (2020); (4) Hogan et al. (2008); (5) Lodieu et al. (2014); (6) Lodieu et al. (2019); (7) Kellogg et al. (2017); (8) Martín et al. (2018); (9) Best et al. (2018); (10) Gaia Collaboration et al. (2021a); (11) Schneider et al. (2017); (12) Pérez-Garrido et al. (2017); (13) Pérez-Garrido et al. (2018); (14) Bouvier et al. (2008); (15) Liu et al. (2016).

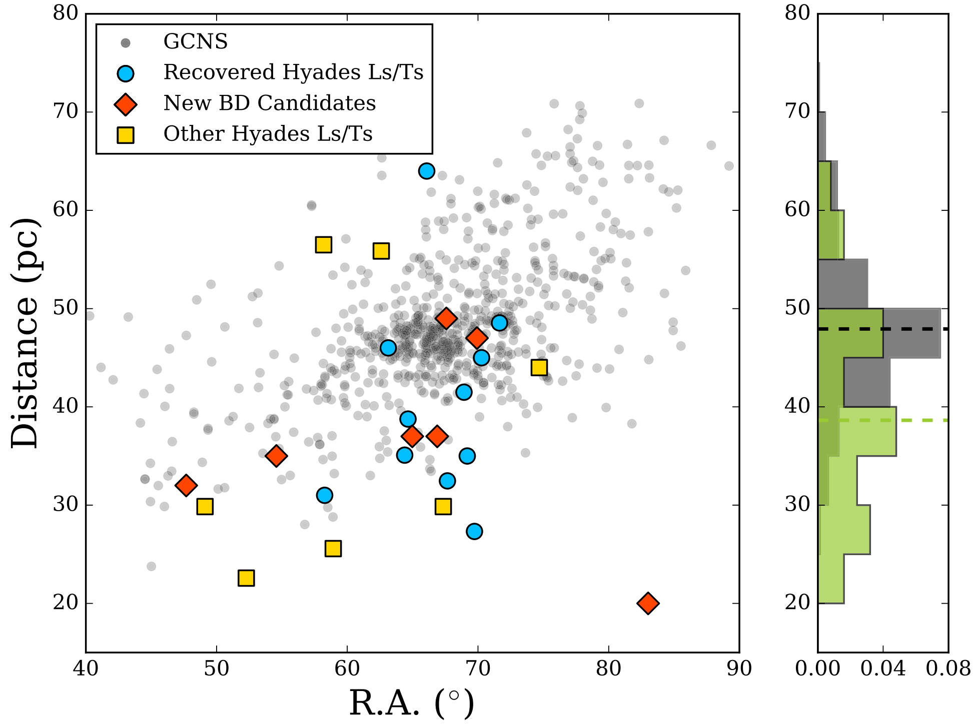

Figure 3. Right ascension vs. distance for the new substellar Hyades candidates in this work (red diamonds), recovered substellar Hyades members from our search (blue circles), and other suggested Hyades L and T members (yellow squares) compared to the 713 Hyades members within a 30 pc radius from the cluster center from the GCNS (Smart & Sarro et al. 2021b). The normalized histograms on the right show the 713 Hyades members from Smart & Sarro et al. (2021b) in gray, and the combined sample of all substellar candidates in green. The median values of each sample are marked with dashed lines.

objects recovered in our search from Table 1 and our seven new candidates from Table 4. To these samples, we include four other L dwarfs from Hogan et al. (2008) with spectral types in Lodieu et al. (2014) or Martín et al. (2018; Hya02, Hya03, Hya08, and Hya11), one additional T dwarf from Bouvier et al. (2008; CFHT-Hy-21), and two Hyades candidates from Zhang et al. (2021; PSO J049.1159+26.8409 and PSO J052.2746+13.3754).

Two previously suggested Hyades members, 2M0429+2437 (Pérez-Garrido et al. 2018) and WISEPA J030724.57+290447.6 (Zhang et al. 2021), we rule out as potential Hyades members based on a reanalysis of their astrometry.

2M0429+2437 (CWISE J042930.33+243749.0) was suggested as a potential Hyades member in Pérez-Garrido et al. (2018), who gave $\mu_\alpha = +45$ mas yr^{-1} and $\mu_\delta = -71$ mas yr^{-1} and indicated a typical proper motion uncertainty of ± 19.3 mas yr^{-1} for each component. They also showed a low-S/N spectrum of this source and gave a spectral type of L6–L8, noting that this source was difficult to classify. CatWISE 2020 (Marocco et al. 2021) gives $\mu_\alpha = +17.2 \pm 14.6$ mas yr^{-1} and $\mu_\delta = -0.9 \pm 15.3$ mas yr^{-1}, which are more precise and significantly different than the values given in Pérez-Garrido et al. (2018). Using the CatWISE 2020 proper motion values of this source, we find a BANYAN Σ Hyades membership probability of 0% for this source. An inspection of optical images of the area around this object shows that its colors are likely influenced by a foreground molecular cloud. We suggest that this object is likely a highly reddened background object. Its nature may be illuminated with a higher-S/N spectrum.

WISEPA J030724.57+290447.6 (CWISE J030724.57+290447.2) was suggested as a very-low-mass Hyades member in Zhang et al. (2021). However, the proper motion components used for this object in that work had significant uncertainties ($\pm$100 mas yr^{-1}). Using the proper motion for this object from our UHS proper motion catalog ($\mu_\alpha = -29.8 \pm 14.7$ mas yr^{-1} and $\mu_\delta = -53.4 \pm 14.6$ mas yr^{-1}) we find a 0% BANYAN Σ Hyades membership probability.

We also exclude CWISE J043803.58+070055.2 (Pérez-Garrido et al. 2018) from our census of potential substellar Hyades members because it is $\gtrsim$30 pc from the Hyades cluster center (see Section 2.1).

The remaining candidates all have BANYAN Σ membership probabilities for the Hyades >0% (Table 6). For this evaluation, we use proper motions with the smallest uncertainties from Liu et al. (2016), Best et al. (2018), Lodieu et al. (2019), Gaia EDR3 (Gaia Collaboration et al. 2021a), or our UHS proper motion catalog. We also use parallactic distances when available, which come from Liu et al. (2016), Lodieu et al. (2019), Best et al. (2020), and Gaia EDR3 (Gaia Collaboration et al. 2021a). When a parallax is not available, we use the *K*-band photometric distance. The general properties of known substellar Hyades candidates are summarized in Table 6. We also include a mass estimate for each object following the method outlined in Section 4.4 using the evolutionary models of Phillips et al. (2020) assuming Hyades membership.

Figure 3 shows the full substellar candidate sample (25 total) versus the 713 member census from Smart & Sarro et al. (2021b). While substellar candidates have been found throughout the cluster, many occupy its nearest edge. As shown in the histograms on the right side of Figure 3, the median distances of the Smart & Sarro et al. (2021b) sample and the combined substellar sample peak at different values. The average distance to members from the Smart & Sarro et al. (2021b) sample is 47.9 pc, while the average distance to the substellar Hyades candidates sample is 38.6 pc. If we exclude objects with low membership probabilities (<50%) from BANYAN Σ (CWISE J031042.59+204629.3 (47.6%), Hya02 (23.9%), CWISE J035304.34+041820.0 (14.7%), and CWISE J053204.60 +111955 (7.1%)), the average distance becomes 39.4 pc. Either way, the average distance difference between substellar candidates and known cluster members indicates that either the substellar sample is contaminated by nearby, unrelated interlopers, the full substellar population of the Hyades has yet to be explored, or some combination of the two. Considering that the search detailed in this work implemented a *J*-mag cut of 17.5 mag, which does not allow for the full extent of spectral types to be probed throughout the entire cluster radius, a deeper search would likely return more substellar Hyades members.

6. Summary

We have presented a search for substellar members of the Hyades based on data from the UHS. We found 25 candidates, 10 of which were previously suggested substellar Hyades members. We classified two known brown dwarfs recovered in our search as potential Hyades members. Of the 13 new discoveries, six objects were found to be unrelated, background cool stars. Five new discoveries are considered strong Hyades candidates, while Hyades membership cannot be ruled out for two additional discoveries. Parallax and radial-velocity measurements will be necessary to confirm Hyades membership for all of these candidates. We also find that the current census of substellar Hyades candidates is likely incomplete, and deeper searches, using the UHS or other surveys, would reveal a more complete accounting of the substellar Hyades population.

This publication makes use of data products from the UKIRT Hemisphere Survey, which is a joint project of the United States Naval Observatory, The University of Hawaii Institute for Astronomy, the Cambridge University Cambridge Astronomy Survey Unit, and the University of Edinburgh Wide-Field Astronomy Unit (WFAU). This project was primarily funded by the United States Navy. The WFAU gratefully acknowledges support for this work from the Science and Technology Facilities Council through ST/T002956/1 and previous grants. The authors acknowledge the support provided by the US Naval Observatory in the areas of celestial and reference frame research, including the USNO's postdoctoral program. This material is supported by the National Science Foundation under grant Nos. 2007068, 2009136, and 2009177. This publication makes use of data products from the *Wide-field Infrared Survey Explorer*, which is a joint project of the University of California, Los Angeles, and the Jet Propulsion Laboratory/California Institute of Technology, and NEOWISE, which is a project of the Jet Propulsion Laboratory/California Institute of Technology. WISE and NEOWISE are funded by the National Aeronautics and Space Administration. Part of this research was carried out at the Jet Propulsion Laboratory, California Institute of Technology, under a contract with the National Aeronautics and Space Administration. The authors wish to recognize and acknowledge the very significant cultural role and reverence that the summit of Maunakea has always had within the indigenous Hawaiian community. We are most fortunate to have the opportunity to conduct observations from this mountain.

Facilities: UKIRT, IRTF.

Software: BANYAN Σ (Gagné et al. 2018), SpeXTool (Cushing et al. 2004).

ORCID iDs

Adam C. Schneider https://orcid.org/0000-0002-6294-5937
Jeffrey A. Munn https://orcid.org/0000-0002-4603-4834
Scott E. Dahm https://orcid.org/0000-0002-2968-2418
Justice Bruursema https://orcid.org/0000-0002-3858-1205
Bryan N. Dorland https://orcid.org/0000-0002-5604-5254
Jacqueline K. Faherty https://orcid.org/0000-0001-6251-0573
Austin Rothermich https://orcid.org/0000-0003-4083-9962
Michael C. Cushing https://orcid.org/0000-0001-7780-3352
Dan Caselden https://orcid.org/0000-0001-7896-5791
Martin Kabatnik https://orcid.org/0000-0003-4905-1370
Arttu Sainio https://orcid.org/0000-0003-4864-5484
Nikolaj Stevnbak Andersen https://orcid.org/0000-0003-4714-3829

References

Allers, K. N., & Liu, M. C. 2013, ApJ, 772, 79
Bensby, T., Feltzing, S., & Lundström, I. 2003, A&A, 410, 527
Best, W. M. J., Liu, M. C., Magnier, E. A., et al. 2015, ApJ, 814, 118
Best, W. M. J., Magnier, E. A., Liu, M. C., et al. 2018, ApJS, 234, 1
Best, W. M. J., Liu, M. C., Magnier, E. A., et al. 2020, AJ, 159, 257
Bouvier, J., Kendall, T., Meeus, G., et al. 2008, A&A, 481, 661
Burgasser, A. J., McElwain, M. W., Kirkpatrick, J. D., et al. 2004, AJ, 127, 2856
Burgasser, A. J., Geballe, T. R., Leggett, S. K., et al. 2006, ApJ, 637, 1067
Burgasser, A. J., & McElwain, M. W. 2006, AJ, 131, 1007
Burgasser, A. J., Liu, M. C., Ireland, M. J., et al. 2008, ApJ, 681, 579
Chambers, K. C., Magnier, E. A., Metcalfe, N., et al. 2016, arXiv:1612.05560
Chiu, K., Fan, X., Leggett, S. K., et al. 2006, AJ, 131, 2722
Cruz, K. L., Burgasser, A. J., Reid, I. N., et al. 2004, ApJL, 604, L61
Cummings, J. D., Deliyannis, C. P., Maderak, R. M., et al. 2017, AJ, 153, 128
Cushing, M. C., Vacca, W. D., & Rayner, J. T. 2004, PASP, 116, 362
De Gennaro, S., von Hippel, T., Jefferys, W. H., et al. 2009, ApJ, 696, 12
Dupuy, T. J., & Liu, M. C. 2012, ApJS, 201, 19
Dye, S., Lawrence, A., Read, M. A., et al. 2018, MNRAS, 473, 5113
Faherty, J. K., Riedel, A. R., Cruz, K. L., et al. 2016, ApJS, 225, 10
Filippazzo, J. C., Rice, E. L., Faherty, J., et al. 2015, ApJ, 810, 158
Gagné, J., Mamajek, E. E., Malo, L., et al. 2018, ApJ, 856, 23
Gaia Collaboration, Babusiaux, C., van Leeuwen, F., et al. 2018, A&A, 616, A10
Gaia Collaboration, Brown, A. G. A., Vallenari, A., et al. 2021a, A&A, 649, A1
Gaia Collaboration, Smart, R. L., Sarro, L. M., et al. 2021b, A&A, 649, A6
Hayashi, C., & Nakano, T. 1963, PThPh, 30, 460
Hodgkin, S. T., Irwin, M. J., Hewett, P. C., et al. 2009, MNRAS, 394, 675
Hogan, E., Jameson, R. F., Casewell, S. L., et al. 2008, MNRAS, 388, 495
Kellogg, K., Metchev, S., Miles-Páez, P. A., et al. 2017, AJ, 154, 112
Kirkpatrick, J. D., Looper, D. L., Burgasser, A. J., et al. 2010, ApJS, 190, 100
Kirkpatrick, J. D., Cushing, M. C., Gelino, C. R., et al. 2011, ApJS, 197, 19
Kirkpatrick, J. D., Kellogg, K., Schneider, A. C., et al. 2016, ApJS, 224, 36
Kirkpatrick, J. D., Gelino, C. R., Faherty, J. K., et al. 2021, ApJS, 253, 7
Kuchner, M. J., Faherty, J. K., Schneider, A. C., et al. 2017, ApJL, 841, L19
Kumar, S. S. 1963, ApJ, 137, 1121
Lawrence, A., Warren, S. J., Almaini, O., et al. 2007, MNRAS, 379, 1599
Lebreton, Y., Fernandes, J., & Lejeune, T. 2001, A&A, 374, 540
Liu, M. C., Dupuy, T. J., & Allers, K. N. 2016, ApJ, 833, 96
Lodieu, N., Boudreault, S., & Béjar, V. J. S. 2014, MNRAS, 445, 3908
Lodieu, N., Smart, R. L., Pérez-Garrido, A., et al. 2019, A&A, 623, A35
Madsen, S., Dravins, D., & Lindegren, L. 2002, A&A, 381, 446
Magnier, E. A., Schlafly, E. F., Finkbeiner, D. P., et al. 2020, ApJS, 251, 6
Marocco, F., Eisenhardt, P. R. M., Fowler, J. W., et al. 2021, ApJS, 253, 8
Martín, E. L., Lodieu, N., Pavlenko, Y., et al. 2018, ApJ, 856, 40
Meingast, S., & Alves, J. 2019, A&A, 621, L3
Pérez-Garrido, A., Lodieu, N., & Rebolo, R. 2017, A&A, 599, A78
Pérez-Garrido, A., Lodieu, N., Rebolo, R., et al. 2018, A&A, 620, A130
Phillips, M. W., Tremblin, P., Baraffe, I., et al. 2020, A&A, 637, A38

Rayner, J. T., Toomey, D. W., Onaka, P. M., et al. 2003, PASP, 115, 362
Reino, S., de Bruijne, J., Zari, E., et al. 2018, MNRAS, 477, 3197
Röser, S., Schilbach, E., Piskunov, A. E., et al. 2011, A&A, 531, A92
Röser, S., Schilbach, E., & Goldman, B. 2019, A&A, 621, L2
Saumon, D., & Marley, M. S. 2008, ApJ, 689, 1327
Schneider, A. C., Windsor, J., Cushing, M. C., et al. 2016, ApJL, 822, L1
Schneider, A. C., Windsor, J., Cushing, M. C., et al. 2017, AJ, 153, 196
Skrutskie, M. F., Cutri, R. M., Stiening, R., et al. 2006, AJ, 131, 1163
Vacca, W. D., Cushing, M. C., & Rayner, J. T. 2003, PASP, 115, 389
Zhang, Z., Liu, M. C., Best, W. M. J., et al. 2021, ApJ, 911, 7